Anomalous light-induced drift of potassium in Ne plus rare-gas mixtures

F. Yahyaei-Moayyed and A. D. Streater
Physics Department, Lehigh University, Bethlehem, Pennsylvania 18015
(Received 11 December 1995)

We report anomalous light-induced drift of potassium vapor in mixtures of Ne with another rare gas. The drift velocity versus laser frequency curve shows a strong deviation from the dispersion curve predicted by the standard theory of light-induced drift based on velocity-independent collision rates. The observed drift velocity versus frequency curves have three zero-crossings. For a qualitative explanation of the results, a strong collision model with velocity-dependent collision rates is used. The partial pressures that cancel normal light-induced drift also provide accurate ratios of cross section for potassium collisions with the various buffer gases. The observation of anomalous light-induced drift in a simple atomic system offers the opportunity to relate the results to potential curves. [S1050-2947(96)02906-X]

PACS number(s): 42.50.Vk, 34.20.Cf, 34.90.+q, 51.20.+d

INTRODUCTION

Light-induced drift (LID) can occur when optically absorbing atoms or molecules immersed in a buffer gas are excited in a velocity selective way. Laser detuning at a frequency that is slightly off the transition resonance excites a velocity class of absorbing atoms. As a result, a flux of excited-state particles and an opposing flux of ground-state particles occur. Because in general the excited-state particles have a different diffusion cross section from the ground-state particles, the excited- and ground-state fluxes do not cancel. The result is a net flux of particles either parallel or antiparallel to the laser beam [1].

Recently, Van der Meer *et al.* [2] observed an anomalous behavior in the dependence of the drift velocity on the laser detuning from resonance. For most atomic and molecular species that could reasonably be described as two-level systems, the drift velocity has a simple dispersionlike shape as a function of the laser detuning. Van der Meer *et al.* [2] found that the LID spectral profile of the C_2H_4 molecule in rare gases on the $(4,1,3)\rightarrow\nu_7(5,0,5)$ rovibrational line had three zeros. Gel'mukhanov and Parkhomenko [3,4] showed that different velocity dependences of the collision cross sections for ground and excited states could yield such a curve, and could even produce drift velocity spectral profiles with up to five zeros. The velocity dependence of the transport collision cross section for some alkali atoms in different quantum states is studied theoretically by Gel'mukhanov and Parkhomenko [5].

In the present paper we report an observation of anomalous LID in an atomic system. We observe additional zero crossings at frequencies on either side of line center for potassium in a mixture of Ne and another rare gas from the group He, Ar, Kr, and Xe.

Yahyaei-Moayyed *et al.* [6] reported normal light-induced drift velocities and diffusion cross-section ratios for potassium excited on the D_1 $(4\,^2S_{1/2}-4\,^2P_{1/2})$ and D_2 $(4\,^2S_{1/2}-4\,^2P_{3/2})$ transitions, in He, Ne, Ar, Kr, and Xe. It was found that $\Delta\sigma/\sigma_g=(\sigma_e-\sigma_g)/\sigma_g$ are positive for all cases except for D_1 excitation in a K-Ne mixture, which had an opposite LID effect. A mixture of Ne and another buffer gas with positive $\Delta\sigma/\sigma_g$ is therefore an ideal experimental condition to observe and study anomalous behavior of LID because the two buffer gases will have opposite LID effects with potassium atoms, so that a mixture of Ne and another buffer gas with certain partial pressures can be chosen such that at particular detunings the drift velocity vanishes, allowing the observation of anomalous LID. The near cancellation of the normal LID by using two species that provide opposite LID effects is somewhat analogous to the cancellation of vibrational and rotational terms that lead to anomalous LID in the molecular cases that have been studied [2,7,8]. In these studies we do not have to rely on a chance cancellation because the buffer-gas partial pressures can be adjusted continuously.

The drift velocities due to anomalous light-induced drift are small and cannot easily be measured by the time-of-flight method used by Atutov *et al.* [9], and Werij and Woerdman [10]. The experimental technique we use to observe this small drift effect is similar to the technique used by Mugglin *et al.* [11] for observing white-light-induced drift, except that fluorescence is used to measure the potassium density instead of transverse absorption of a probe laser.

EXPERIMENT

The experimental setup is shown in Fig. 1. The test cell is made of borosilicate glass. The capillary has an inner diameter of 4.0 mm and a length of 11 cm. The cell is coated with a monolayer silane nonstick surface in order to prevent adsorption of potassium atoms onto or into the glass walls. The coating is deposited by rinsing the cell walls with a solvent containing a few drops of hexadecyltrichlorosilane. This coating is essentially the same as the coating used in Ref. [6] [6,12] for normal LID measurements, except that the polymer chain has sixteen hydrocarbon units instead of eighteen.

A buffer-gas mixture of ~4–10 Torr is admitted into the cell, which results in homogeneous widths ~0.1 GHz. These pressures are chosen to preserve velocity selectivity, since the Doppler width is ~0.5 GHz, while still assuring relatively slow diffusion in the main capillary.

The potassium metal in the side appendix (see Fig. 1) is heated, creating a vapor that diffuses into the main tube at the T intersection. In the experiment, the potassium density is low enough ($\sim 10^6$ cm^{-3}) that the vapor cloud is very

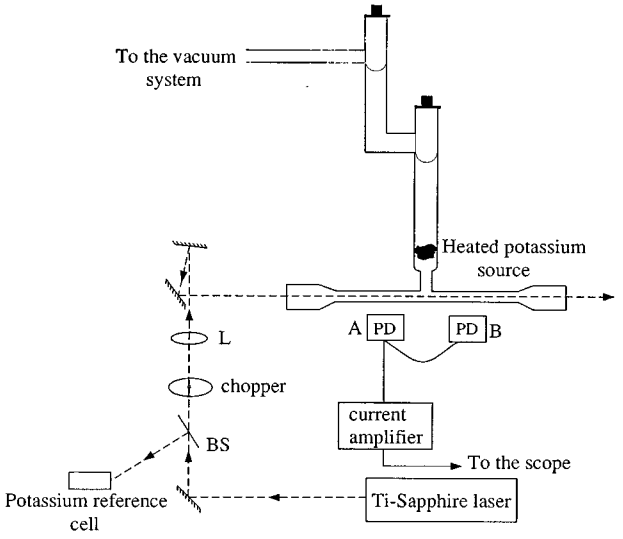

FIG. 1. Schematic diagram of the experimental setup. PD, L, and BS, represent photodiode, lens, and beam splitter, respectively.

optically thin for the LID laser beam passing through the main tube.

In the absence of LID (beam blocked), a symmetrical potassium vapor cloud is formed by atoms diffusing into the T intersection of the cell and then symmetrically outward into both sides of the main capillary. The density decreases on either side of the T intersection, due to either a gradual chemical loss by reactions with impurities or occasional sticking to the wall, or due to the boundary condition that the density is zero where the capillary opens into the wide window regions that do not contain potassium atoms. (The large-volume window regions are far removed from the source, and potassium atoms that diffuse through the main tube spread out into these regions and are eliminated by occasional sticking or chemical loss.) When the laser beam is introduced, atoms are pushed or pulled, causing the cloud to become asymmetrical. If the beam is kept on, the cloud eventually reaches a new asymmetrical steady state. It is this change to a new asymmetrical configuration that we measure.

The beam from a tunable, stabilized, single-mode Ti-sapphire laser, pumped by an argon ion laser, is focused at the chopper wheel and collimated by lens L. The photodiode detectors A and B are used to detect the fluorescence of potassium atoms at points placed symmetrically on either side of the T intersection. The photodiodes A and B are wired to switches such that the signals $-A$, B, or the difference signal $B-A$ can be detected. The signal is then amplified by a current amplifier and displayed on a digital oscilloscope. By recording $B-A$ directly, noise due to fluctuations in the laser power is minimized.

After the laser beam is admitted to the cell at time $t=0$, light-induced drift occurs and the potassium atoms are pushed or pulled through the buffer-gas mixture, causing the asymmetry in the density of potassium atoms to build up. As a result of LID pushing (pulling), fluorescence signal B is increasing (decreasing) and fluorescence signal A is decreasing (increasing), and consequently, the difference signal $B-A$ is increasing (decreasing) in time. The density profile,

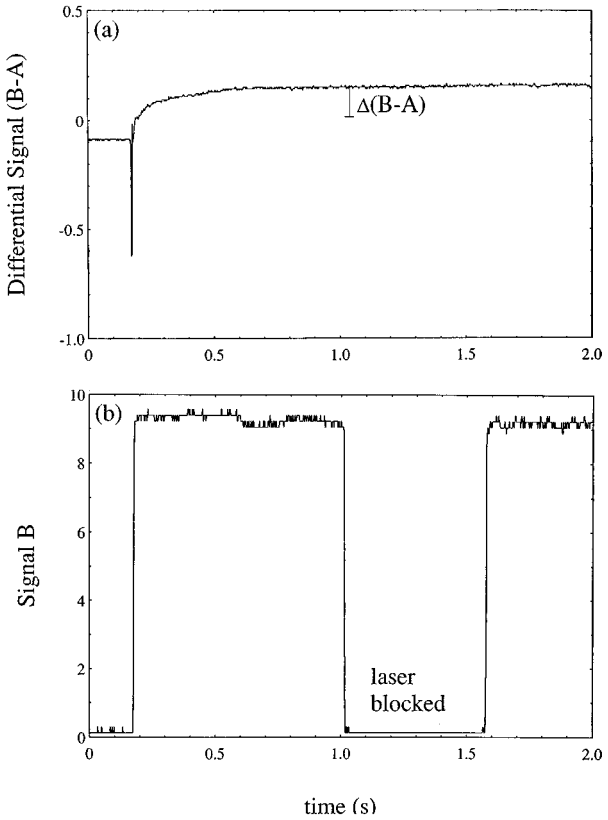

FIG. 2. Typical experimental fluorescence signals (a) B-A and (b) B in the case of a mixture of Ar (partial pressure 0.5 Torr) and Ne (partial pressure 4.0 Torr). In this case the laser is detuned 0.6 GHz to the red side of the maximum fluorescence point for a vacuum potassium vapor reference cell. The slight change in unaveraged signal B after the beam is admitted is lost in the noise, but is easily observed in the difference signal, which is an average of eight repeated signals. About $\frac{1}{2}$ of the signal B represents scattered light, and $\frac{1}{2}$ represents fluorescence.

and therefore the signals, will reach a steady state if the beam has been on for sufficient time. Even if the cloud is not initially exactly symmetric for $\nu_d=0$ (e.g., due to impurities in the coating on one side of the T intersection), the change upon admitting the laser will be in the same sense and of approximately the same magnitude. Care is taken to first balance the signals A and B by adjusting the position of photodiodes A and B before introducing buffer gas into the cell, and with the laser tuned to direct resonance (thus eliminating LID). Then the buffer-gas mixture is introduced to the cell and the signals $B-A$ and B are recorded as the laser beam is detuned to different frequencies. Figure 2 shows a typical example of the time-dependent signals (a) $B-A$ and (b) B as functions of time, after the beam is admitted, for the case of an Ar-Ne mixture. The signal $B-A$ is averaged over eight repetitive sweeps while the signal B is not averaged. (Note also that the signal B is blocked while the beam is still on between $t=1$ s and 1.6 s, in order to record the baseline.) The signal B is also recorded for a large laser detuning, where the excitation of atoms by the laser beam is zero. Therefore, we know the amount of scattering of the laser beam, which we call B_0. Then we subtract the scattering from any measurement of signal B, in order to obtain a fluorescence signal that

is directly proportional to the potassium density. The change of the signal $(B-A)/(B-B_0)$ from early to late times, which we shall call $\Delta(B-A)/(B-B_0)$, is equal to the relative change in the difference of potassium concentrations in the right- and left-hand sides of the cell, which we can write $(\Delta n_B-\Delta n_A/n_B \cong 2\Delta n/n_B$ if $\Delta n_B \cong -\Delta n_A \equiv \Delta n$. To first order (for small ν_d), this signal should be proportional to ν_d, the drift velocity.

In order to observe the anomalous light-induced drift (ALID) effect, we must find partial pressures of Ne and another buffer gas such as He, Ar, Kr, or Xe, that cancel the normal LID effect. We have an initial guess for the proper ratio of the rare-gas pressures based on the ratio of cross sections for K-Ne, and K-He, Ar, Kr, or Xe from the normal LID experiments [6]. Because the collision rates of the Ne-buffer gas mixture are the sum of the rates for both gases, we have

$$\nu_d \propto \frac{(\gamma_e)_{\rm tot}-(\gamma_g)_{\rm tot}}{(\gamma_g)_{\rm tot}}, \tag{1}$$

where

$$(\gamma_e)_{\rm tot}=\gamma_{e1}+\gamma_{e2}=n_1\sigma_{e1}\overline{\nu_1}+n_2\sigma_{e2}\overline{\nu_2},$$

$$(\gamma_g)_{\rm tot}=\gamma_{g1}+\gamma_{g2}=n_1\sigma_{g1}\overline{\nu_1}+n_2\sigma_{g2}\overline{\nu_2}, \tag{2}$$

where $\overline{\nu_i}$ are the thermal relative velocities. We should therefore obtain $\nu_d=0$ when

$$\frac{n_2}{n_1}=\frac{\overline{\nu_1}}{\overline{\nu_2}}\frac{(\sigma_{e1}-\sigma_{g1})}{(\sigma_{g2}-\sigma_{e2})}. \tag{3}$$

With this initial guess, the cell is first filled to pressure P_1 with the heavier rare gas. While the laser beam is detuned to the frequency at which the drift velocity is maximum for normal LID, the manifold before the cell is filled with the lighter buffer gas to a total pressure slightly below the desired value $P_1(1+n_2/n_1)$. Then the cell valve is opened for a short time. This establishes a pressure equilibrium with a ratio slightly smaller than the desired ratio. The signal $B-A$ is monitored, and the direction of the LID is easily observed. We repeat this procedure with a slightly higher pressure in the manifold until we find the experimental ratio that nearly cancels the normal LID. To fine-tune the pressure ratio to exactly cancel the normal LID, we now gradually increase the ratio n_2/n_1 by holding the valve open to allow diffusion to further mix the lighter buffer gas into the cell, until the difference signal $B-A$ becomes flat, indicating no drift. Now by varying the laser frequency, ALID can be observed.

EXPERIMENTAL RESULTS

The anomalous light-induced drift effect is studied for potassium in Ne and one of the other rare gases, He, Ar, Kr, or Xe. In all cases we report the behavior of $\Delta(B-A)/(B-B_0)$ for initial and late times t, which represents the relative change in density

$$\frac{n_B(t)-n_B(0)-(n_A(t)-n_A(0))}{n_B(t)} \approx \frac{\Delta n_B(t)-\Delta n_A(t)}{n_B(t)}. \tag{4}$$

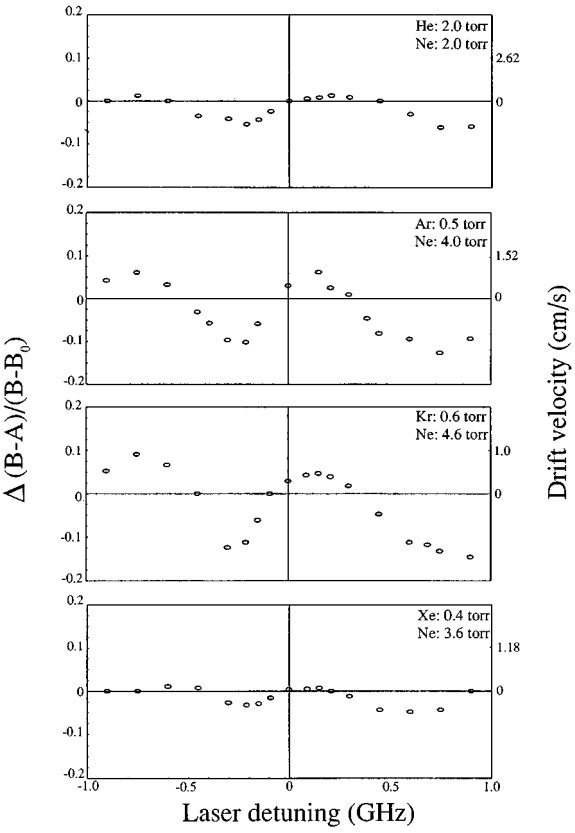

FIG. 3. Experimental results for the fluorescence difference signal $\Delta(B-A)/(B-B_0)$ vs the laser detuning (from the fluorescence maximum for a vacuum potassium vapor reference cell) for He-Ne, Ar-Ne, Kr-Ne, and Xe-Ne mixtures.

For small drift velocities, the signal decays to the steady state on two time scales. The shorter time scale is on the order of $\Delta z/\nu_d$, where Δz is the lateral shift of the cloud edges between the initial symmetrical density profile and the shifted steady-state profile. The second and longer time scale is due to the effect of the boundary condition at the T intersection, and is on the order of the cloud width divided by the drift velocity. This longer decay time is more sensitive to the dynamics of the source and stem tube, so we chose to measure the change due to the faster decay, which was measured at about $t=600$ ms. There is some uncertainty in the assignment of this change, which we estimate to be 10%.

The drift velocity ν_d can be obtained from the measured signal, using a simple model, which we describe below. The reported laser powers are the average of powers measured before and after the cell with a calibrated photodiode power meter. Pressures are measured with a capacitance manometer, which is accurate to 0.1 Torr.

Results for He-Ne, Ar-Ne, Kr-Ne, and Xe-Ne mixtures are shown in Fig. 3. The measured laser powers, which differ from day to day due to laser alignment instabilities, were 108, 204, 159, and 103 mW, for the He-Ne, Ar-Ne, Kr-Ne, and Xe-Ne mixtures, respectively. The case of He-Ne mixture is noteworthy because a qualitative discrepancy was reported in Yahyaei-Moayyed *et al.* [6] between experimental and theoretical results for normal LID in K-He. A positive value was reported for a relative change in diffusion cross section, $(\sigma_e-\sigma_g)/\sigma_g=\Delta\sigma/\sigma_g$, while calculations [6,13,14]

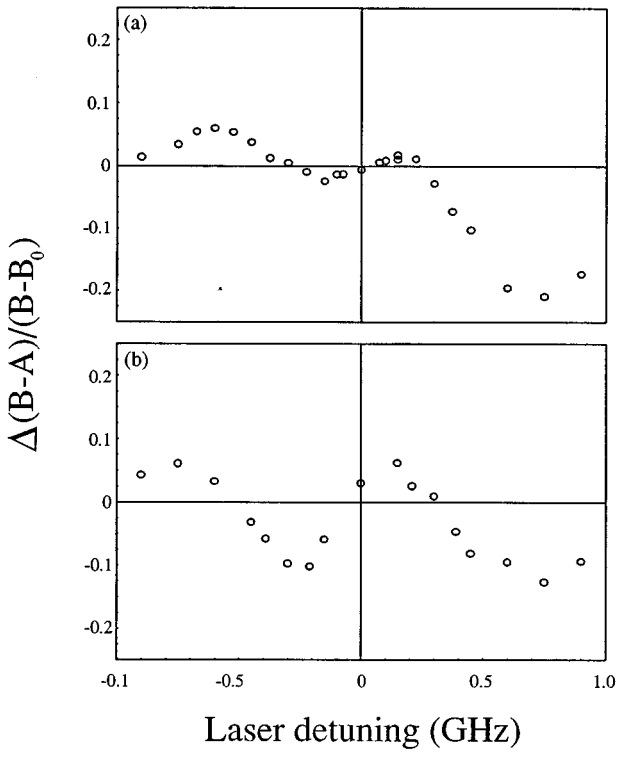

FIG. 4. Experimental results for $\Delta(B-A)/(B-B_0)$ vs the laser detuning for Ar-Ne mixture. In (b) a slight amount of Ne is added to the mixture, producing a more balanced profile (also shown in Fig. 3).

based on available potential curves predicted a negative value for $\Delta\sigma/\sigma_g$. The fact that we could cancel the normal LID for D_1 excitation with a He-Ne mixture supports the experimental result of Yahyaei-Moayyed *et al.* [6] that, for the K-He case, $\Delta\sigma/\sigma_g>0$.

In Figs. 4(a) and 4(b) the effect of changing the ratio of the Ar-Ne mixture is demonstrated. Figure 4(a) indicates that Ar has a dominant effect because a pushing effect for red-side detuning of the Doppler wing is predominant. Figure 4(b), which is the case of an Ar-Ne mixture in Fig. 3, is the result when a small amount of Ne is added to the cell. The ALID velocity vs frequency curve is more balanced in Fig. 4(b). A mixture with more Ar than Fig. 4(a) would result in a normal LID signal with a dispersive shape that has a larger amplitude (in drift velocity) and is positive (pushing) for red detunings. For the case of pure Ar, for example, the drift velocities are much larger ($\sim m/s$), and the drift velocity frequency curve is dispersive [6].

The difference between the pressure ratios for Figs. 4(a) and 4(b) is very small. The valve separating the cell and the manifold was held open (under total pressure equilibrium) for a few seconds, allowing additional Ne to diffuse into the cell. The zeroing of the drift velocity can, in fact, provide an extremely sensitive measure of the ratios of the cross-section differences in Eq. (3). The measured pressure ratios that cancel the normal LID and the ratios predicted by the previous measurements of Yahyaei-Moayyed *et al.* [6] are shown in Table I. Although the agreement does not at first appear good, the previous results are in agreement with these new results. The large relative uncertainties in the prediction based on the earlier experimental cross sections are a result

TABLE I. The calculated and experimental ratios of the Ne partial pressure to the other rare-gas partial pressure that lead to a cancellation of normal LID. The total experimental pressure is also indicated.

	$P_{Ne}/P_{rare\ gas}$		Total pressure
	From Ref. [6]	This experiment	(Torr)
He-Ne	0.8±3.9	1.0± 0.2	4.0±0.1
Ar-Ne	3±10	8.3±0.7	9.0±0.1, 9.6±0.1
Kr-Ne	3±9	7.7±1.5	5.2±0.1
Xe-Ne	5±14	9±3	4.0±0.1

of the differences appearing in Eq. (3). The new measurements directly measure these difference ratios with a higher accuracy. In fact, these measurements are limited primarily by the uncertainty in the pressure measurements, which are limited due to the precision of the gauge. The partial pressures are also uncertain due to diffusive mixing of the buffer gases by an unknown amount during the time that the valve is open, just after pressure equilibrium is established, when letting in the lighter buffer gas. A direct measurement of the partial pressures in the cell would eliminate these uncertainties, allowing a very sensitive measurement of these thermally averaged cross-section difference ratios. More accurate measurements are planned for the future, which should put stringent constraints on the potassium–rare-gas potential curves.

Model for potassium cloud evolution

The potassium cloud spreads due to diffusion during propagation along the capillary. A simple model for the evolution of the density $n(z,t)$ of K atoms is to assume one-dimensional diffusion, constant drift velocity, and a constant chemical loss rate. The potassium cloud evolution is then governed by the equation

$$\frac{\partial n}{\partial t}=D\,\frac{\partial^2 n}{\partial z^2}-\frac{\partial(n\nu_d)}{\partial z}-\alpha n, \quad z\neq 0, \tag{5}$$

where D, ν_d, and α are the diffusion coefficient, drift velocity, and chemical loss rate, respectively. In steady state, and assuming a fixed density at $z=0$ and an infinite tube, the distribution of K atoms, $n(z)$, is described by Atutov *et al.* [15]:

$$n(z)=\begin{cases} n_0\,\exp(z/l_1), & z<0 \\ n_0\,\exp(-z/l_2), & z>0 \end{cases} \tag{6}$$

where l_1 and l_2 are characteristic lengths defined as

$$(l_1)^{-1}=\sqrt{\left(\frac{\nu_d}{2D}\right)^2+\frac{\alpha}{D}}+\frac{\nu_d}{2D},$$
$$(l_2)^{-1}=\sqrt{\left(\frac{\nu_d}{2D}\right)^2+\frac{\alpha}{D}}-\frac{\nu_d}{2D}. \tag{7}$$

If the photodiodes A and B are at equal distance d from T intersection of the experimental cell, one finds

$$\frac{n_B - n_A}{n_B} = \frac{2\Delta n}{n_B} = \frac{\exp(-d/l_1) - \exp(-d/l_2)}{\exp(-d/l_2)}. \quad (8)$$

The appropriate value for the chemical loss decay rate α is determined approximately by the observed spatial extent of the cloud (for $\nu_d = 0$). Although the size of the cloud may also be partly determined by the boundary condition imposed by the window regions, which do not contain potassium vapor, it is expected that the results would be fairly similar if these boundary conditions were included, especially for the change over the shorter decay time, as discussed above. We therefore set the chemical loss rate used to the value $\alpha = D/l^2$.

In the experiment, the detector positions are chosen to be approximately at $\pm l$, where l is the cloud width in the absence of drift. This provides the maximum sensitivity for measuring small changes in the density due to LID.

From Eqs. (7) and (8) we can find the relation predicted by this model, between $(\Delta n_B - \Delta n_A)/n_B \approx 2\Delta n/n_B$ [equal to the signal ratio $\Delta(B-A)/(B-B_0)$] vs the drift velocity. We can then use this relationship to determine the drift velocity vs frequency detuning from the experimental results shown in Figs. 3 and 4. The experimental maximum value of 0.2 is obtained for $2\Delta n/n_B$. In this range, Eqs. (7) and (8) predict that the drift velocity is fairly linear with the density change, so that the results shown in Figs. 3 and 4 are approximately the drift velocity vs detuning profiles. The approximate drift velocity scales are shown in the right-hand sides of Fig. 3.

A second simple model that is related to the model used by Atutov [15] (described above) is to assume a constant source rather than a fixed density in the center. For our cell, where the source is in a reservoir connected to the main tube by another narrow stem tube at the T intersection, the model of a constant source may be slightly better. This model is constructed by dropping the fixed density boundary condition at $z = 0$, and adding a source $s\,\delta(z)$ to Eq. (5), where s is the source strength (particles/sec). The steady-state solutions are still the same as Eq. (6), with

$$n_0 = \left[2D \sqrt{\frac{\nu_d^2}{4D^2} + \frac{\alpha}{D}} \right]^{-1} s.$$

The time evolution, however, is slightly different for the two cases.

Figure 5 shows results of a numerical solution of Eq. (5) with the added source term, for the density profile in space at several different times for parameters modeling an Ar-Ne mixture. Figure 6 shows the theoretical evolution of the density in time for two fixed detector positions (3 and -3 cm with respect to T intersection). The difference signal $B-A$ is also shown. This signal can be qualitatively compared to Fig. 2. In particular, note that the model is in good agreement with respect to the short relaxation time scale for the signal. It is interesting to note that both experimentally, and in the results of the model, this relaxation time scale is relatively independent of the drift velocity. The reason for this is that the short relaxation time scale is approximately the distance of the cloud shift Δz divided by the drift velocity. The positional shift Δz is also proportional to the drift velocity, so that the drift velocity cancels out of the expression for the relaxation time scale. For small drift, for our range of parameters, this time scale is roughly $l^2/2D = 1/2\alpha$.

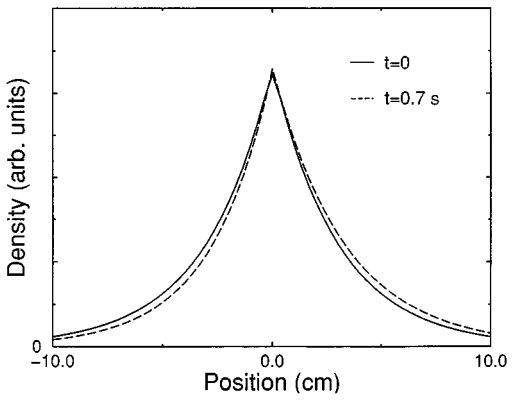

FIG. 5. Model results for the potassium cloud evolution for different times in the case of the Ar-Ne mixture where $D = 45.3$ cm^2/s, $\nu_d = 1.52$ cm/s, and $\alpha = 5.0$ s^{-1}.

Strong collision model with velocity-dependent collision rates

Velocity-dependent rate equation models have been well established for modeling the normal LID process. The strong collision model has been found to be a good approximation for drift velocity calculations [16]. In this section we use a modified strong collision model to qualitatively predict the anomalous drift velocity vs frequency behavior that is in agreement with the experimental observations. The model, similar to that used in Ref. [17], assumes four levels: $4\,^2S_{1/2}(F=1)$, $4\,^2S_{1/2}(F=2)$, $4\,^2P_{1/2}$, and $4\,^2P_{3/2}$, as described in Ref. [6]. This can account for fine-structure collisions between the excited levels and hyperfine pumping of the lower levels. In Refs. [6] and [17] we assumed that the collision rates were constant. Here, in order to model anomalous LID, we allow the strong collision rates to depend on the absolute value of the velocity component along the direction of light propagation.

We begin by assuming a linear speed dependence for the strong collision rates, for each gas, as follows:

$$\gamma_{ij} = \gamma_{ij}^0 \left(1 + m_{ij} \frac{|v| - v_B}{v_B} \right).$$

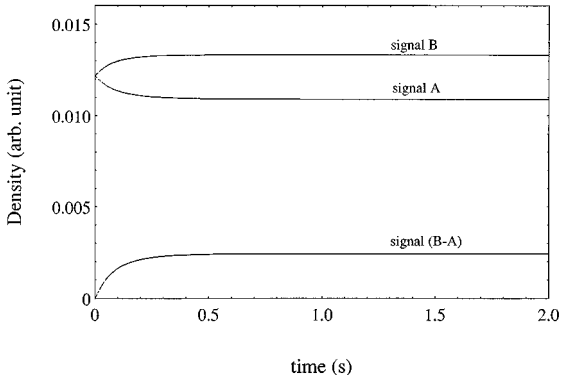

FIG. 6. Theoretical potassium cloud evolution in time, for parameters modeling an Ar-Ne mixture, for two fixed positions 3 cm (signal B) and -3 cm (signal A). The difference of the two signals $(B-A)$ is also shown. Parameters are the same as in Fig. 5.

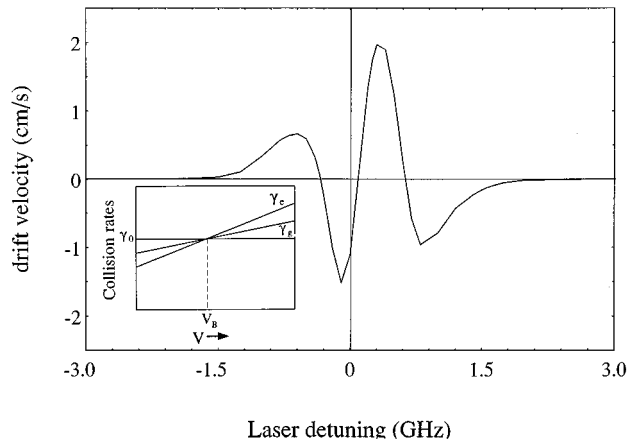

FIG. 7. Results of a modified strong collision model, assuming a linear dependence for collision rates on the absolute value of the velocity component along the direction of light propagation for the case of relative slopes $m_e - m_g = 0.01$. The laser detuning is from the center of the $4\,^2S_{1/2}(F=2) - 4\,^2P_{1/2}$ hyperfine transition. The maximum fluorescence point occurs at a detuning 0.14 GHz, which corresponds to zero in Figs. 3 and 4. Other parameters model the experiment for the Xe-Ne mixture.

Here γ_{ij} is the strong collision rate from level $i \rightarrow j$ (for $i \neq j$, it is assumed that velocity-changing and fine-structure-changing collision rates are the same), γ_{ij}^0 are the velocity-independent rates obtained from the normal LID experiment [6], ν_B is the average velocity of potassium atoms, and m_{ij} is the relative slope. The assumption of linear velocity dependence of the collision rates is the simplest velocity dependence that qualitatively explains the ALID experimental results. We can also consider this assumption to be the first term in a Taylor expansion of the collision rate about the thermal velocity.

We assume that the two hyperfine ground-state levels have the same slope, since the ground and excited potential curves with a particular buffer gas should be essentially identical, and we denote this slope m_g. For simplicity, let us also assume that the fine-structure-level strong collision rates have equal slopes, which we denote m_e (for strong collisions that involve a state change as well as those that do not). Assuming identical excited-state relative slopes is a crude approximation, but the model results are only sensitive to the slopes out of the $4\,^2P_{1/2}$ level, which is directly excited by the laser. The solutions from this model indicate that we can obtain qualitative behavior similar to the experimental observations for the drift velocity as a function of detuning if $m_e > m_g$. This is shown in Fig. 7 for parameters modeling a Xe-Ne mixture. Note that there are four extrema and three zeros in the drift velocity spectral profile, starting with a positive drift velocity at detunings far to the red side of resonance, changing to negative for smaller detuning in this side, and with an opposite behavior on the blue side of the resonance. Calculations show that if $m_e < m_g$, then the sign of the drift velocity is reversed from above.

In each case we have assumed that both Xe and Ne have the same relative slopes (m_e, m_g), which presumably represent weighted averages of the effective slopes of the two buffer gases. Also, the strong-collision model calculations show that the ALID velocity depends primarily on the difference of the relative slopes, $m_e - m_g$, but is fairly independent of the individual value for m_e and m_g.

These results are for parameters (e.g., the experimental laser power and temperature) that model the experiments. The thermally averaged diffusion cross sections of the rare gases have been taken from Ref. [6], except that the ground-state cross sections for K-Ne and K-Xe have been modified slightly to reflect the new experimental information in Table I.

DISCUSSION

The overall sign of the drift velocity vs laser frequency curve has already demonstrated a trend that for the rare-gas–neon mixtures, the velocity dependence of the collision rates have slopes that are greater for the excited $4\,^2P_{1/2}$ level than for the ground $4\,^2S_{1/2}$ level. Gel'mukhanov and Parkhomenko [5] have recently calculated ALID velocities for other alkali atoms from available potential curves. While these potential curves are not sufficiently accurate for predicting LID velocities in detail [6], the calculated ALID profiles for the other alkali-metal atoms from Ref. [5] are qualitatively similar to these experimental results for potassium. Higher derivatives or moments in the velocity dependence can affect other details of the drift velocity vs frequency curve.

By comparing the measured ALID velocities for different Ne–rare-gas mixtures, we can hope to discover effects that are specific to the buffer gases. Compare the case of a He-Ne mixture, for example, to the case of Xe-Ne. The laser intensities are roughly the same, and the anomalous drift velocities are about 3–4 times larger for the He-Ne case. For the Xe-Ne case the buffer gas consists mostly of Ne, while for the He-Ne case the proportions of the two gases are about equal. Calculations based on the strong collision model indicate that, for the Ne-Xe mixture, the magnitude of the anomalous drift velocity is more sensitive to the Ne slopes than the Xe slopes, while for the He-Ne mixture the results are relatively sensitive to the He slopes. The larger drift for the He-Ne case would therefore seem to indicate that the difference of the effective relative slopes of the collision rate is larger for He than for Ne. If we compare the Xe-Ne and He-Ne cases further, we observe that for the rare-gas compositions that best balance out the normal LID, the zero crossings are further apart for the He-Ne mixture. Further analysis may reveal that this indicates a different velocity dependence in the He and Xe collision rates. Before we investigate these possibilities we plan to carefully develop the experimental apparatus in order to obtain higher-resolution data.

CONCLUSION

We observed anomalous light-induced drift for K in Ne–rare-gas mixtures. A model for the evolution of the potassium cloud in the cell is used to relate the observed density changes to drift velocities. The drift velocities are on the order of a few cm/s, and in this range the drift velocity is approximately a linear function of the observed density changes. A modified strong collision model is discussed in which linear velocity dependences for the collision rates are

assumed. The calculations agree qualitatively with the observations, and indicate that the effective relative slope for the velocity dependence is greater for the excited-state collision rate than for the ground state. The magnitude of the difference is roughly $m_e - m_g \sim 0.01$. Further analysis and higher-resolution data may reveal other details of the alkali-metal–rare-gas interaction.

ACKNOWLEDGMENTS

We thank A. P. Hickman and Amy Van Engen for valuable discussions. Acknowledgment is made to the Donors of The Petroleum Research Fund, administered by the American Chemical Society, for partial support of this research.

[1] F. Kh. Gel'mukhanov and A. M. Shalagin, Pis'ma Zh. Eksp. Teor. Fiz. **29**, 773 (1979) [JETP Lett. **29**, 711 (1979)].
[2] G. J. Van der Meer, J. Smeets, S. P. Pod'yachev, and L. J. F. Hermans, Phys. Rev. A **45**, 1303 (1992).
[3] F. Kh. Gel'mukhanov and A. I. Parkhomenko, Phys. Lett. **162A**, 45 (1992).
[4] F. Kh. Gel'mukhanov and A. I. Parkhomenko, Zh. Eksp. Teor. Fiz. **102**, 424 (1992) [Sov. Phys. JETP **75**, 225 (1992)].
[5] F. Kh. Gel'mukhanov, and A. I. Parkhomenko, J. Phys. B **28**, 33 (1995).
[6] F. Yahyaei-Moayyed, A. P. Hickman, and A. D. Streater, J. Phys. B **29**, 435 (1996).
[7] P. O. Chapovsky, G. J. van der Meer, J. Smeets, and L. J. F. Hermans, Phys. Rev. A **45**, 8011 (1992).
[8] G. J. van der Meer, J. Smeets, E. R. Eliel, P. L. Chapovsky, and L. J. F. Hermans, Phys. Rev. A **47**, 529 (1993).
[9] S. N. Atutov, S. Lesjak, S. P. Prodjachev, and A. M. Shalagin, Opt. Commun. **60**, 41 (1986).
[10] H. G. C. Werij and J. P. Woerdman, Phys. Rep. **169**, 145 (1988).
[11] D. T. Mugglin, A. D. Streater, S. Balle, and K. Bergmann, Opt. Commun. **104**, 165 (1993).
[12] D. L. Angst and G. W. Simmons, Langmuir **7**, 2236 (1991).
[13] A. P. Hickman, D. T. Mugglin, and A. D. Streater, Opt. Commun. **102**, 281 (1993).
[14] W. A. Hamel, J. E. M. Haverkort, H. G. C. Werij, and J. P. Woerdman, J. Phys. B **19**, 4127 (1986).
[15] S. N. Atutov, I. M. Ermolaev, and A. M. Shalagin, Zh. Eksp. Teor. Fiz. **92**, 1215 (1987) [Sov. Phys. JETP **65**, 679 (1987)].
[16] J. E. M. Haverkort, H. G. C. Werij, and J. P. Woerdman, Phys. Rev. A **38**, 4054 (1988).
[17] A. D. Streater and J. P. Woerdman, J. Phys. B **22**, 677 (1989).